HYDROLOGICAL PROCESSES
Hydrol. Process. (2012)
Published online in Wiley Online Library
(wileyonlinelibrary.com) DOI: 10.1002/hyp.9386

Climate change sensitivity assessment of streamflow and agricultural pollutant transport in California's Central Valley using Latin hypercube sampling

Darren L. Ficklin, Yuzhou Luo and Minghua Zhang*

Department of Land, Air and Water Resources, University of California, Davis, CA 95616, USA

Abstract:

Bracketing the uncertainty of streamflow and agricultural runoff under climate change is critical for proper future water resource management in agricultural watersheds. This study used the Soil and Water Assessment Tool (SWAT) in conjunction with a Latin hypercube climate change sampling algorithm to construct a 95% confidence interval (95CI) around streamflow, sediment load, and nitrate load predictions under changes in climate for the Sacramento and San Joaquin River watersheds in California's Central Valley. The Latin hypercube algorithm sampled 2000 combinations of precipitation and temperature changes based on Intergovernmental Panel on Climate Change projections from multiple General Circulation Models. Average monthly percent changes of the upper and lower 95CI limits compared to the present-day simulation and a statistic termed the "*r*-factor" (average width of the 95CI band divided by the standard deviation of the 95CI bandwidth) were used to assess watershed sensitivities. 95CI results indicate that streamflow and sediment runoff in the Sacramento River watershed are more likely to decrease under climate change compared to present-day conditions, whereas the increase and decrease for nitrate runoff were found to be equal. For the San Joaquin River watershed, streamflow slightly decreased under climate change, whereas sediment and nitrate runoff increased compared to present-day climate. Comparisons of watershed sensitivities indicate that the San Joaquin River watershed is more sensitive to climate changes than the Sacramento River watershed, which is largely caused by the high density of agricultural land. Copyright © 2012 John Wiley & Sons, Ltd.

KEY WORDS SWAT; climate change; agricultural pollution; streamflow; sediment; nitrate

Received 26 July 2011; Accepted 11 April 2012

INTRODUCTION

The uncertainty associated with climate change has been described as "persistent," "deep," and "irreducible" (Preston, 2005). These uncertainties exist at the global (e.g. climate feedback processes and climate sensitivity) and regional scale (e.g. greenhouse gas emissions and population growth). Many General Circulation Models (GCMs) have been created to investigate the effects of increasing greenhouse gas concentrations on the climate. These studies indicate an increase in global mean temperature, on average, between 1.1 and 6.4 °C compared to the 20th century average temperature depending on the greenhouse gas emission scenario [Intergovernmental Panel on Climate Change (IPCC), 2007]. End of 21st century GCM projections for California, which is the area of this study, show an increase in air temperature of 1 to 4.5 °C (e.g. Maurer, 2007; Cayan *et al*., 2008; Ficklin *et al*., 2012a). Changes in precipitation, however, are more speculative than temperature, especially for smaller regions where GCMs predict a wide range of positive and negative precipitation projections compared to present-day totals. In California, for example, GCMs project a wide array of precipitation projections, with a median projection of an 8% decrease from present-day precipitation totals (Cayan *et al*., 2008; Ficklin *et al*., 2012a). Any change in temperature and precipitation will affect the hydrological cycle, resulting in a large variation of streamflow and agricultural pollutant fate and transport. Climate change uncertainties create a range of challenges for scientific investigations and decision-making processes. Ideally, information from each plausible climate change scenario should be used to make informed risk management decisions at the watershed level (Preston, 2005).

The integration of risk management considerations is not a trivial matter, particularly for systems with multiple uncertainties. Stochastic simulations such as Monte Carlo and Latin hypercube analysis are useful for achieving such integration for complex modelling of the environment. Baalousha (2006) used a modified Latin hypercube sampling (LHS) technique with success to assess groundwater pollution risk. Seibert and McDonnell (2010) used a Monte Carlo technique to bracket the 95% confidence interval (95CI) of streamflow simulations from different land-cover regimes in Oregon, USA. Many other studies use LHS as a way to collect information about the hydrological characteristics of a region for a wide array of model input parameter sets (e.g. Abbaspour *et al*., 2004; Yang *et al*., 2008). For this study, we employ the LHS method because of its widespread use in uncertainty analyses and ease of use, as it is included in

*Correspondence to: Minghua Zhang, Department of Land, Air and Water Resources, University of California, Davis, CA 95616, USA.
E-mail: mhzhang@ucdavis.edu

the popular Soil and Water Assessment Tool Calibration Uncertainty Program (SWAT-CUP; Abbaspour *et al*., 2007). Furthermore, in comparing uncertainty analysis methods, Yu *et al*. (2001) and Melching (1992) investigated the efficiency of different uncertainty analysis sampling methods, concluding that LHS could generate representative sampling more efficiently than the Monte Carlo technique due to uniform sampling of the parameter space.

Although a plethora of studies have investigated the changes in surface runoff and streamflow associated with climate change, only a few have investigated how warmer climates and precipitation changes could affect water quality (e.g. Cruise *et al*., 1999; Chaplot, 2007; Ficklin *et al*., 2010). The relationship between precipitation changes and increased agricultural pollutant runoff is easily understood, as rainfall impacts and runoff are the driving mechanisms for pollutant transport within watersheds. The relationship between temperature increases and agricultural pollutant runoff is not as easily understood due to changes in evapotranspiration and irrigation water use. Our previous study (Ficklin *et al*., 2010) found that agricultural pollutant runoff decreased with increases in temperature.

The goal of this study is to assess the sensitivity of climate change on the Sacramento and San Joaquin River watersheds using a stochastic method with bracketed output from multiple GCMs and emission scenarios to determine the 95CI of streamflow and agricultural pollutant transport (sediment and nitrate) using SWAT (Arnold *et al*., 1998). These watersheds drain into the Sacramento–San Joaquin Delta (Delta), which in recent years has seen an appreciable decline in aquatic species, attributed in part to an increase of in-stream agricultural pollution (Werner *et al*., 1999). Therefore, this type of analysis is extremely beneficial to all parties interested in the health and security of the Delta. The probabilistic climate change assessment offers a useful framework for managing decision-making events by uncertainty.

METHODS

Study sites

Sacramento River watershed. The Sacramento River watershed area, as defined by this study, is approximately 23 300 km^2 (Figure 1). The Sacramento River monitoring gauge maintained by the United States Geological Survey (USGS) at Freeport, CA (USGS gauge #11447650), is the outlet of the simulated watershed. The watershed boundary is defined by the discharge inlets listed in Table I. The western side is bordered by the Black Butte Dam on Stony Creek; the eastern side is bordered by the Oroville Dam on the Feather River, the Yuba River at Marysville USGS gauge, the Camp Far West Dam on Bear River, and the Folsom Dam on the American River; the northern side is bordered by the Shasta Dam on the Sacramento River and the Whiskeytown Dam on Clear Creek. The study area includes the majority of agricultural land in the northern Central Valley, from Sacramento, CA, to Red Bluff, CA. The majority of the land use in the study area is rangeland composing approximately 62% of the total watershed area, whereas agricultural land composes approximately 33% of the total area. The remaining 5% contains urban land use, waterways/wetlands, and forested areas.

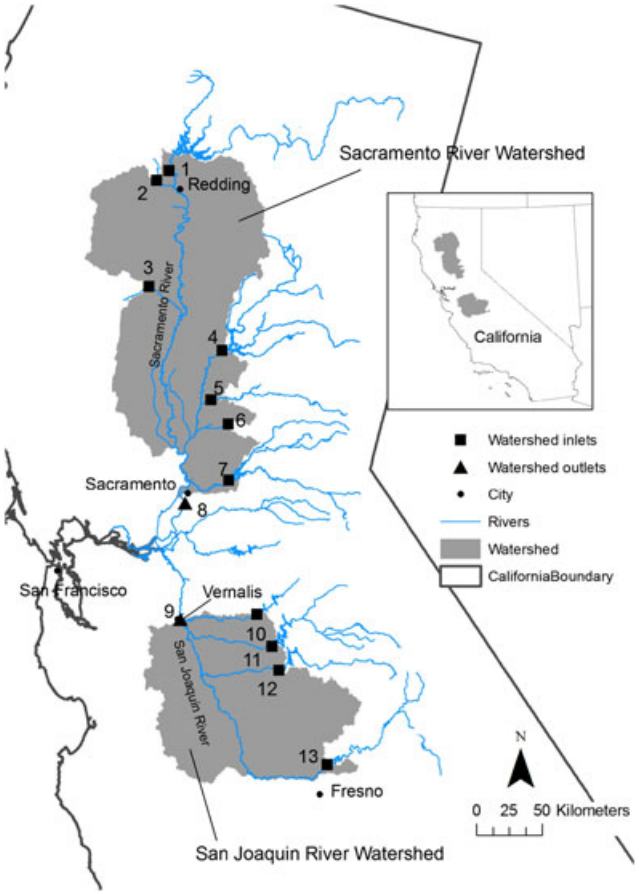

Figure 1. Sacramento and San Joaquin River watersheds modelled in the study. The numerical value refers to the ID in Table I

The Sacramento Valley has a Mediterranean climate characterized by hot summers and mild winters, with an average temperature ranging from 4 °C in the winter to above 32 °C in the summer (Guo *et al*., 2007). Mean annual precipitation ranges from 36 to 64 cm, with most of the precipitation occurring between November and April. The soils of the valley are mostly fine grained with low permeability (Troiano *et al*., 2001). Water requirement for crops grown on 8500 km^2 is dependent on irrigation from surface water or groundwater (DWR, 1998). Human intrusion for urban and agricultural uses has greatly disrupted the natural hydrology in this region.

San Joaquin River watershed. The San Joaquin River watershed, as defined by this study, is 14983 km^2, with approximately 66% of the total area in the San Joaquin Valley, 15% in the Coastal Range, and 19% in the Sierra Nevada mountains (Figure 1). The USGS monitoring site at Vernalis (USGS gauge #11303500) is the outlet for the watershed. The USGS gauges of the upper San Joaquin River at the Friant Dam, the upper Merced River at the

DOI: 10.1002/hyp

Table I. Locations of watershed inlets and outlets for the Sacramento and San Joaquin River watersheds

ID	USGS ID# or CA DWR ID	River	Gauge name	Latitude	Longitude	Inlet (I) or outlet (O)
1	SHA	Sacramento River	Shasta Dam	40.60	−122.44	I
2	11372000	Clear Creek	Whiskeytown Dam transfer	40.52	−122.53	I
3	BLB	Stony Creek	Black Butte Dam	39.81	−122.33	I
4	ORO	Feather River	Oroville Dam	39.52	−121.55	I
5	11421000	Yuba River	Yuba River—Marysville	39.18	−121.52	I
6	CFW	Bear River	Camp Far West Dam	39.05	−121.32	I
7	AMF	American River	Folsom Dam	38.68	−121.18	I
8	11447650	Sacramento River	Sacramento River—Freeport	38.45	−121.50	O
9	11303500	San Joaquin River	San Joaquin River—Vernalis	37.68	−121.27	O
10	11302000	Stanislaus River	Goodwin Dam	37.85	−120.64	I
11	11289650	Tuolumne River	La Grange Dam	37.67	−120.44	I
12	11270900	Merced River	Merced Falls Dam	37.52	−120.33	I
13	11251000	San Joaquin River	Friant Dam	36.98	−119.72	I

Note: The ID value refers the numerical value on Figure 1.

Merced Falls Dam, the upper Tuolumne River at the La Grange Dam, and the upper Stanislaus River at the Goodwin Dam are the inlets for the watershed (Figure 1, Table I). The watershed is highly agricultural; of the total cropland in the study area, 38% is covered by fruits and nuts, 36% by field crops (corn, tomatoes, pumpkins, watermelon, asparagus, cotton, beans, etc.), 17% by truck, nursery, and berry crops, and 4% by grain crops (DWR, 2007).

The San Joaquin Valley has a Mediterranean climate with hot, dry summers and cool, wet winters. Average annual rainfall is approximately 20 to 30 cm, with most of the precipitation falling between November and April. Average temperatures range from 11 °C in the winter to 25 °C in the summer (NOAA, 2008). Due to the arid climate, agriculture in the San Joaquin Valley critically depends on irrigation. Farmers in the San Joaquin Valley use a combination of groundwater and surface water to meet irrigation needs.

SWAT model description

The Soil and Water Assessment Tool is a model designed to simulate watershed processes at a river-basin scale (Arnold *et al*., 1998) that has been successfully applied in many environments (Gassman *et al*., 2007). SWAT simulates the entire hydrological cycle, including surface flow, lateral soil flow, evapotranspiration, infiltration, deep percolation, and groundwater return flows. For this study, surface runoff was estimated using the Soil Conservation Service Curve Number (CN), an empirical parameter for predicting runoff based on soil properties and land use (SCS, 1984), and evapotranspiration was estimated using the Penman–Monteith method (Penman, 1956; Monteith, 1965). Water within the soil column can be removed by evaporation or plant water uptake, deep percolation for aquifer recharge, or lateral movement in the soil column for streamflow contribution. Groundwater return flow is estimated based on the groundwater balance, where shallow and deep aquifers can contribute to streamflow. A temperature index–based approach is used to estimate snow accumulation and snowmelt processes. Irrigation was automatically scheduled and based on a soil water deficit, where water is added to the soil column when the soil water is below user-defined percentage of field capacity. For this study, irrigation occurs only when the soil water is at 85% of field capacity. Fertilizer was automatically added to the top layer of the soil based on a user-defined nitrogen stress threshold, which is a fraction of potential plant growth. Anytime the actual plant growth falls below this threshold, the model will automatically apply fertilizers. The nitrogen stress threshold used in this study was 0.95. We assume that growers will irrigate and apply nitrogen to the soil using the same thresholds as the present-day figures, and thus, the irrigation and nitrogen stress values remained constant for all simulations. Input data for SWAT include spatially distributed information basin topography, soil properties, land use/land cover, and climate time-series data. The model was run at a monthly time step. A full description of SWAT can be found in Neitsch *et al*. (2005).

SWAT model input data

Compiled from state and government agency databases were SWAT input parameter values from topography, land use/land cover, soil, and climate data. Data extracted from the Environmental Protection Agency include 1:250 000-scale quadrangles of land use/land cover data, 1:24 000-scale digital elevation models, and 1:100 000-scale stream network data from the National Hydrography Dataset. Cropland was defined based on the land-use survey database completed by the California Department of Water Resources (DWR) during 1996–2004. Cropland information will be assumed to have remained unchanged since the date of survey completion. Land use/land cover remained constant throughout the climate change simulations. Soil properties in the watershed were extracted from the 1:24 000 Soil Survey Geographic database. Daily weather data, including precipitation and minimum and maximum temperatures, were retrieved from the California Irrigation Management Information System.

DOI: 10.1002/hyp

Irrigation was automatically simulated by SWAT based on the soil water deficit. Depending on the subwatershed, irrigation water was extracted from the nearby reach or a source outside the watershed. Fertilization was automatically applied based on a plant growth threshold.

Climate change projections

Recent hydrological studies incorporate projections from GCMs, downscaled to a higher resolution for California (e.g. Maurer and Duffy, 2005; Maurer, 2007; Cayan *et al*., 2008). These studies show general agreement with temperature increases but great variability in projected precipitation for California. Consequently, no GCM should be considered superior to others in predicting California precipitation, and any projection should therefore be regarded as equally plausible. For this study, we will use the upper limit for IPCC temperature projections of +6.4 °C and a ±20% precipitation change compared to the present-day climate. These values bracket the range of plausible climate change scenarios for LHS.

Latin hypercube sampling

The LHS technique is a type of stratified Monte Carlo simulation first suggested by McKay *et al*. (1979). It has been used in a wide array of research topics for sensitivity and uncertainty analysis (Iman *et al*., 1981; Helton and Davis, 2003). The idea of LHS depends on the subdivision of a sampling space (in this case, temperature and precipitation) into N_s numbers of non-overlapping segments with equal probability. LHS then draws a sample from each segment. Once the segments are defined, each individual parameter is randomized until a value that lies within each probability segment is found. Each round of sampling chooses randomly in a way that every interval contains one sample. The random numbers for each parameter are then combined with the random numbers from other parameters such that all possible combinations of segments are sampled (Baalousha, 2006). LHS can be executed based on the following formula:

$$x_{ij} = F^{-1}\left(\frac{\pi_{j(i)} - U_{ij}}{N_s}\right) \tag{1}$$

where $\pi_{j(i)}$ is the random permutation of 1 to n, where n is the total number of realizations; F^{-1} is the inverse cumulative probability density function; U_{ij} is a $U[0,1]$ random variable; N_s is the number of segments; j is 1,2,... k, where k is the dimension input of vector X. For this project, the number of realizations (model runs) and segments is 2000, and temperature and precipitation are the parameters being sampled. The sampling range for temperature and precipitation is +0 to 6.4 °C and −20 to +20% compared to the present-day climate, respectively. A sampling of 2000 would subdivide the temperature and precipitation ranges into 0.003 °C and 0.02%, respectively, and therefore, the selection of 2000 segments will cover all potential temperature and precipitation projections. We assume the relationship between temperature and precipitation to be independent. Precipitation and temperature are negatively correlated, as dry conditions favour more sunshine and less evaporative cooling, whereas wet days are cooler than dry days (Trenberth and Shea, 2005). However, the purpose of this study is to assess the changes of streamflow and agricultural pollutant transport using every plausible combination of temperature and precipitation. Including the relationship between temperature, precipitation, and relative humidity was beyond the scope of this study. Additionally, we assume that all temperature and precipitation pairings are equally plausible. It is important to note that an assessment of model sensitivity to climate change does not necessarily provide a projection of the likely consequences (Ficklin *et al*., 2009). However, such studies provide valuable insights into the sensitivity of hydrological changes to changes in climate (Arnell and Liv, 2001).

Calculation of the 95CI

After the LHS is performed, the temperature and precipitation values were input into SWAT to simulate streamflow and agricultural pollutant transport. In total, there were 2000 simulations for each scenario, with varying precipitation and temperature inputs. The 95CI was calculated from the output of these simulations based on the algorithm developed by Abbaspour *et al*. (2007). This algorithm is normally used for hydrological model calibration, where the 95CI is calculated from changes in model parameters on an uncalibrated model. The 95CI would then give a result of parameter uncertainty, and subsequent steps would decrease this uncertainty by narrowing the parameter ranges. For this study, temperature and precipitation are the only variables changed and are varied upon a calibrated SWAT model. Therefore, the 95CI calculated in our study is only from changes in precipitation and temperature, which we assume to be a climate change sensitivity assessment.

In the first step, a sensitivity matrix, J, is computed using

$$J_{i,j} = \frac{\Delta g_i}{\Delta b_j} \tag{2}$$

where i is the number of rows (equal to all possible combinations), j is the number of columns (precipitation and temperature), g is the objective function value [in this case, the Nash–Sutcliffe coefficient (NS; Nash and Sutcliffe, 1970)] of the climate change simulation compared to the present-day climate simulation, and b is the climate change parameter (temperature or precipitation). The Hessian matrix, H, is then calculated by following the Gauss–Newton method:

$$H = J^T J \tag{3}$$

Then, based on the Cramer-Rao theorem (Press *et al*., 1992), an estimate of the lower bound of the parameter covariance matrix, C, is calculated from

DOI: 10.1002/hyp

$$C = s_g^2 \left(J^T J\right)^{-1} \tag{4}$$

where s_g^2 is the variance of the climate change simulations compared to the present-day climate from the n runs. The estimated standard deviation and 95CI interval of a parameter, b_j, are calculated from the diagonal elements of C from

$$s_j = \sqrt{C_{jj}} \tag{5}$$

$$b_{j,\text{upper}} = b_j^* + z * s_j \tag{6}$$

$$b_{j,\text{lower}} = b_j^* - z * s_j \tag{7}$$

where b_j^* is the parameter b for the solution with no temperature and precipitation change, and z is the upper critical value of the t-distribution with $n-1$ degrees of freedom (1999 for this study).

Statistical analyses

Absolute percent change compared to the long-term average (also termed "upper and lower limit") was calculated for each month for all model output. *T*-tests for dependent samples were performed on streamflow, sediment, and nitrate scenarios at the 0.05 significance level.

RESULTS AND DISCUSSION

SWAT model calibration and validation

The calibration and validation procedures can be found in Luo *et al*. (2008) for the San Joaquin River watershed and Ficklin *et al*. (2012b) for the Sacramento River watershed. Both models were previously calibrated and validated for streamflow, sediment loads, and nitrate loads measured at USGS gauges located within the Sacramento and San Joaquin River watersheds. At the Freeport USGS site for the Sacramento River watershed (Figure 1, Table I), the NS coefficients for validation were 0.86 for streamflow, 0.64 for sediments, and 0.51 for nitrate (Ficklin *et al*., 2012b). Average monthly streamflow, sediment loads, and nitrate loads during the present-day simulation were 778 m^3/s, 165 833 tons/month, and 1 502 220 kg/month, respectively. At the Vernalis USGS site for the San Joaquin River watershed (Figure 1, Table I), the NS for the validation period was 0.95 for streamflow, 0.74 for sediments, and 0.85 for nitrate (Luo *et al*., 2008). Average monthly streamflow, sediment loads, and nitrate loads during the present-day simulation were 121 m^3/s, 23 324 tons/month, and 278 735 kg/month, respectively. Both models provided satisfactory simulation results in estimating the temporal trend and variation of streamflow and agricultural pollutant loads, and therefore, the models were deemed suitable for evaluating the sensitivity to climate change.

Latin hypercube sampling

Figure 2 displays the results of the Latin hypercube temperature and precipitation sampling for the 2000 SWAT model runs. As shown from the even scattering of data points in Figure 2, the sampling did a satisfactory job at pairing nearly all possible combinations of precipitation and temperature. Most importantly, the temperature (+0 and 6.4 °C) and precipitation (−20% and +20%) extremes were sufficiently sampled (Figure 2).

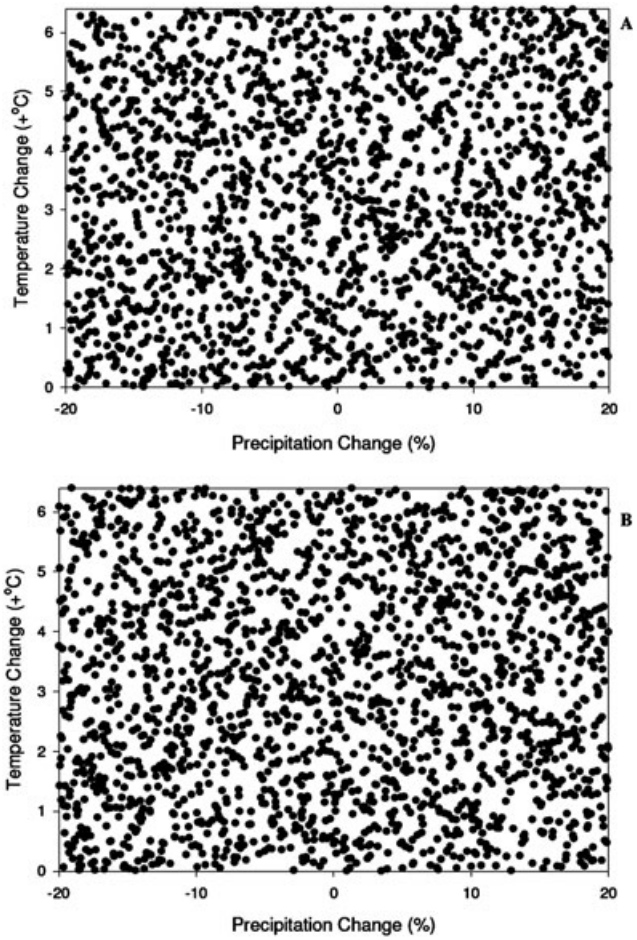

Figure 2. Scatterplots showing the Latin hypercube sampling of the Sacramento River watershed (A) and the San Joaquin River watershed (B)

Hydrological and agricultural pollutant changes

Presented streamflow, sediment load, and nitrate load results are from the Sacramento River—Freeport and the San Joaquin River—Vernalis USGS gauging stations and are considered the outlet for their respective watersheds (Figure 1, Table I). For both watersheds, the streamflow is highly controlled by the upstream reservoir releases, and therefore, any changes in model output compared to present-day simulations are dependent on hydrological conditions within the watersheds and not from changes in reservoir management.

Streamflow. For the Sacramento River watershed streamflow, *t*-tests indicate that the upper and lower 95CI limits were not significantly different ($p < 0.05$) from present-day streamflow rates, which is due to the managed reservoir releases into the watershed (Figure 3). The average monthly absolute percent change for the 95CI upper limit was 3%, whereas the lower limit was 10% compared to the present-day streamflow (Table II). This

DOI: 10.1002/hyp

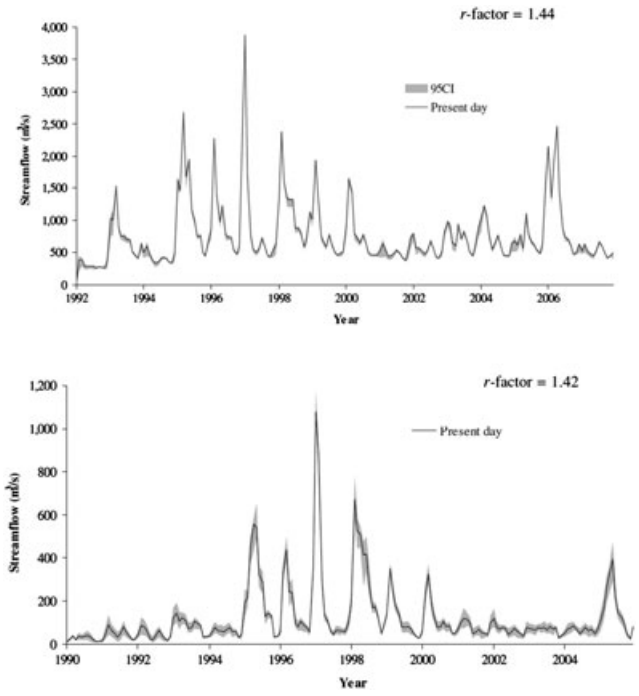

Figure 3. Streamflow 95% confidence intervals from the climate change simulations for the Sacramento (top) and San Joaquin River (bottom) watersheds

indicates that long-term streamflow in the Sacramento River watershed is more likely to decrease with changes in climate. The change in the 95CI lower limit was greater than the upper limit for each month, with the smallest difference occurring during the dry season months of August through October (Table II). The largest decrease occurred in December with a 15% change compared to present-day streamflow, whereas the smallest decrease occurred during October with a 5% change.

Flood weirs on the Sacramento River muted the change in the upper limit of 95CI. Six major flood control structures are located on the Sacramento River. When the river is above a particular discharge value, water spills over the weir structures, capturing streamflow that would have originally remained in the river. The weirs transport water into wetlands, other streams, or completely out of the modelled watershed. Therefore, increases in streamflow from precipitation increase may be captured by the flood weirs. These flood weir structures are accounted for within the SWAT model (Ficklin *et al.*, 2012b). Within the model, if the streamflow is above a certain discharge (from Feyrer *et al.*, 2006), the water is routed to the diversion destination.

For the San Joaquin River watershed streamflow, the overall mean monthly absolute percent change values for the 95CI upper and lower limits were 27% and 28% compared to the present-day climate, respectively (Figure 3, Table II). *T*-tests indicate that both 95CI limits were not significantly different ($p < 0.05$) from the present-day streamflow rates, which is, again, due to the managed reservoir releases into the watershed. There was high variability within seasons. Generally, the upper limit of the 95CI was greater in January through June compared to the lower limit. Conversely, the lower limit of the 95CI was

Table II. Monthly upper and lower confidence percent changes compared to the present-day simulation for streamflow, sediment loads, and nitrate loads for the Sacramento and San Joaquin River watersheds

			Month												
			J	F	M	A	M	J	J	A	S	O	N	D	Average
Sacramento River watershed	Streamflow	Upper limit (%)	4.2	5.1	2.5	2.6	2.5	2.7	3.7	1.3	1.4	1.5	4.2	4.6	3.0
		Lower limit (%)	13.2	14.2	9.4	10.7	10.0	8.1	7.0	5.1	4.8	4.6	11.6	15.4	9.5
	Sediment load	Upper limit (%)	36.2	34.2	43.0	27.0	13.7	12.4	10.1	6.9	8.2	8.5	12.6	21.4	19.5
		Lower limit (%)	30.2	32.5	21.9	21.6	26.1	27.0	25.4	23.3	16.2	18.4	31.9	34.7	25.8
	Nitrate Load	Upper limit (%)	19.4	31.6	16.2	5.2	7.3	9.2	12.5	6.3	4.3	5.9	15.8	19.4	12.8
		Lower limit (%)	20.7	17.0	14.9	12.5	16.2	13.1	11.2	7.9	6.5	5.5	11.6	13.3	12.5
San Joaquin River watershed	Streamflow	Upper limit (%)	29.5	26.9	25.8	20.7	29.3	42.5	35.9	24.9	24.7	22.4	19.4	24.0	27.2
		Lower limit (%)	26.5	26.2	26.8	23.9	23.9	31.2	30.8	34.7	39.0	29.8	21.4	23.9	28.2
	Sediment load	Upper limit (%)	65.5	57.0	55.3	51.2	94.1	164.6	135.1	66.9	39.7	39.1	48.0	62.0	73.2
		Lower limit (%)	51.7	48.6	48.7	46.7	48.8	45.8	50.6	56.1	56.7	40.5	43.9	49.2	48.9
	Nitrate Load	Upper limit (%)	37.2	28.8	25.7	20.3	9.1	3.1	21.3	61.1	70.6	31.5	9.9	21.6	28.3
		Lower limit (%)	27.5	33.8	42.1	39.1	30.6	35.0	25.2	17.2	16.2	12.7	12.7	17.5	25.8

DOI: 10.1002/hyp

generally greater than the upper limit from July through December. The largest absolute percent change increase and decrease were 42% and 39% and occurred in June and September, respectively (Table II).

Sediment Loads. The average monthly absolute percent change for the Sacramento River watershed sediment load was 20% for the upper 95CI limit and 26% for the lower 95CI limit; these were found to be significantly different from present-day sediment loads ($p > 0.05$) (Figure 4, Table II). This indicates that there is a high variability in sediment loads, with a tendency to decrease under climatic changes. The monthly sediment load absolute percent change for the Sacramento River watershed indicates that there is likely to be an increase for late winter/early spring and decreases for the rest of the year. This is potentially caused by the presence of large precipitation events during late winter/spring. The largest increase and decrease occurred during March and September, with an absolute percent change of 43% and 34%, respectively (Table II).

The average monthly absolute percent change for the San Joaquin River watershed sediment load 95CI upper limit was 73% and 49% for the lower limit compared to the present-day simulation, indicating a tendency for an increase in sediment runoff under climatic change (Figure 4, Table II). However, the upper and lower 95CIs were not significantly different ($p < 0.05$) from the present-day simulations. Sediment load increased for every month except for September and October (Table II). The largest increases occurred during the late spring/early summer. The lower 95CI limits remained consistent for each month, with a standard deviation of approximately 4.6%. The largest sediment load increase occurred in June with an absolute percent change of 165%, and the largest sediment load decrease occurred in September with a 57% decrease. It is worthy to note that, although large sediment loads are observed during the wet season, high loads are also found in the irrigation season.

For the winter and spring months, large changes in sediment loads are expected. Sediment is largely generated by winter and spring precipitation events, and therefore, any change in those events will have a large effect on the amount of sediment transported out of the watershed. For the summer months, sediment movement is transported by sediment runoff from irrigation applications and streambed erosion. If the streamflow energy is low enough, sediment can be deposited within the streams, resulting in a decrease in sediment loads. Therefore, the high correlation ($r > 0.90$) between changes in sediment loads and streamflow is to be expected.

Nitrate Loads. The Sacramento River watershed average monthly absolute percent change in nitrate was 13% for the 95CI upper limit and 13% for the 95CI lower limit compared to the present-day simulation (Figure 5, Table II). *T*-tests indicate, however, that the 95CI upper limit was not significantly different ($p > 0.05$), whereas the 95CI lower limit was ($p < 0.05$). The monthly absolute percent changes showed high variability compared to

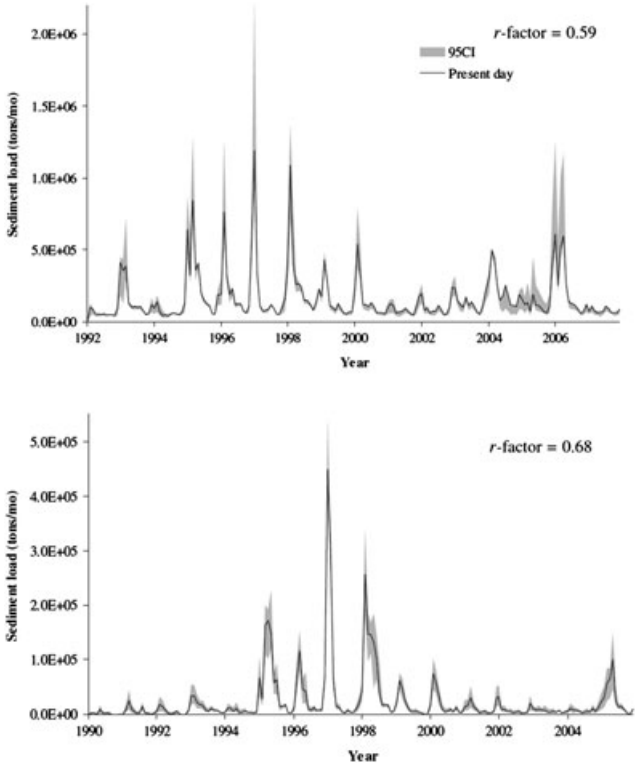

Figure 4. Sediment load 95% confidence intervals from the climate change simulations for the Sacramento (top) and San Joaquin River (bottom) watersheds

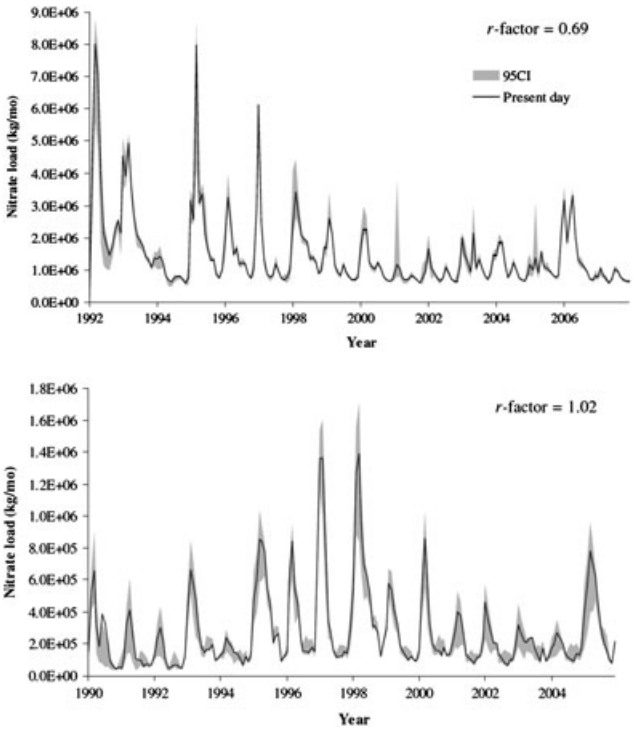

Figure 5. Nitrate load 95% confidence intervals from the climate change simulations for the Sacramento (top) and San Joaquin River (bottom) watersheds

DOI: 10.1002/hyp

present-day nitrate loads, with no consistent increase or decrease throughout the year. Nitrate loads generally had the tendency to increase during the late fall and winter months and to decrease during the summer months. The largest increase was 32% and occurred in February, whereas the largest decrease was 21% and occurred in January (Table II). This result is expected, as an increase or decrease in rainfall will result in corresponding increases or decreases in nitrate runoff.

The average monthly absolute percent change for the San Joaquin River watershed nitrate loads was 28% for the 95CI upper limit and 26% for the lower limit (Figure 5). Both 95CI limits were found to be significantly different ($p < 0.05$). This suggests a slight tendency for nitrate to increase with climatic changes. The largest absolute percent change increase and decrease were 71% and 42% and occurred in September and March, respectively (Table II). Table II indicates a strong seasonal variation in nitrate runoff. During the early spring and summer, nitrate loads have the tendency to decrease, whereas in the late summer and winter months, they have the tendency to increase. This can be attributed to changes in plant growth. Our previous study (Ficklin *et al*., 2009) found that the watershed-wide average leaf area index with elevated temperature peaked up to two months relative to the present-day climate. This resulted in changes in evapotranspiration as well as changes in agricultural management.

Nitrate load results are associated with dissolved-phase nitrate only, and thus, all nitrate yield is water associated. Therefore, nitrate runoff is dependent on the hydrological balance, the quantities present in the soil either from natural sources or from fertilizer inputs, and the degree to which they are removed by plants at the site (Ferrier *et al*., 1995). Changes in surface water runoff appeared to be the most significant factor in fertilizer runoff changes in a study by Mander *et al*. (2000). In our study, changes in nitrate runoff for both watersheds were moderately correlated (r greater than 0.50, but less than 0.75; $p < 0.05$) with changes in streamflow. Annual fertilizer use did not significantly decrease under climate change. However, it was found that less fertilizer was applied during the summer months for both watersheds due to the shift in plant growth patterns from an increase in air temperature. In our previous study (Ficklin *et al*., 2009), we showed that watershed-wide average leaf area index in the San Joaquin River watershed shifted ahead one month with a 1.1 °C air temperature increase and three months with a 6.4 °C air temperature increase. A shift in plant growth results in a shift in fertilizer use, thus reducing the amount used in the summer months.

Comparison and differences in watershed sensitivities. Before discussion, it is important to note the differences in volumes in both watershed outputs. Whereas the San Joaquin River watershed may have a larger absolute percent difference (representing sensitivity), the Sacramento River watershed may have overall larger output caused by the difference in watershed size. Therefore, the watersheds must be compared by normalized statistics.

The 2000 Latin hypercube simulations for each watershed were used for the calculation of the 95CI. The average width of the 95CI band divided by the standard deviation of the 95CI bandwidth (termed the "*r*-factor" by Abbaspour *et al*., 2004) is a good indicator to use for the comparison of watershed sensitivities. Generally, sensitivity decreases as the *r*-factor decreases, indicating a small 95CI width. The streamflow *r*-factors for the Sacramento and San Joaquin watersheds were 1.44 and 1.42, indicating that the streamflow within both watersheds was equally sensitive to climate change (Figure 3). This is most likely caused by the large effect of reservoir releases into the watersheds. Based on the absolute percent change sediment load statistics, the San Joaquin River watershed is nearly twice as sensitive as the Sacramento River watershed (Table II). The sediment load *r*-factors were 0.59 for the Sacramento River watershed and 0.68 for the San Joaquin River watershed, which represents a higher sensitivity for the San Joaquin River watershed (Figure 4). Compared to the San Joaquin River watershed, more sediment may be transported out of the Sacramento River watershed between the months of January and April whereas less may be transported during the rest of the year compared to the present-day climate simulations. For nitrate loads, the absolute percent change statistics indicate that the San Joaquin River watershed is more sensitive than the Sacramento River watershed (Table II). The nitrate load *r*-factors were 0.69 for the Sacramento River watershed and 1.02 for the San Joaquin River watershed, indicating a higher sensitivity of nitrate runoff to climate change for the San Joaquin River watershed compared to the Sacramento River watershed (Figure 5).

Climate change sensitivity differences between the two watersheds can be attributed to two factors: differences in land use and soil properties. Precipitation was varied by the same percentage for both watersheds and was assumed not to be a factor. The differences between land use and soil properties between the watersheds may seem nominal but can be large when extrapolated over large areas. A comparison of the agricultural land acreage from DWR land-use data indicates that the San Joaquin River watershed contains approximately twice as much agricultural land than the Sacramento River watershed. The San Joaquin watershed area is approximately 8500 km^2 less than the Sacramento River watershed, leading to a higher agricultural land density. A difference in agricultural acreage will have large effects on (1) irrigation water use, (2) evapotranspiration water loss, (3) agricultural management practices leading to susceptibility of field erosion, and (4) a higher density of fertilizer use, leading to increased nitrate runoff susceptibility.

There are several differences in soil properties that may lead to the differences with climate change sensitivities. SWAT uses the Modified Universal Soil Loss Equation (MUSLE; Williams, 1975) to estimate sediment yield from each subbasin:

DOI: 10.1002/hyp

$$Sed = 11.8 * \left(Q_{\text{surf}} * q_{\text{peak}} * area_{\text{HRU}}\right)^{0.56} * K_{\text{usle}} * C_{\text{usle}} * P_{\text{usle}} * LS_{\text{usle}} * CFRG \quad (8)$$

where *Sed* is the sediment yield on a given day (metric tons), Q_{surf} is the surface runoff volume (mm H_2O/ha), q_{peak} is the peak runoff rate (m^3/s), $area_{\text{HRU}}$ is the area of the Hydrologic Response Unit (ha), K_{usle} is the USLE soil erodibility factor [0.013 metric ton m^2 h / (m^3-metric ton cm)], C_{usle} is the USLE cover and management factor, P_{usle} is the USLE support practice factor, LS_{usle} is the USLE topographic factor, and *CFRG* is the coarse fragment factor. The slopes of the two watersheds are approximately equal, and therefore, the LS_{usle} will be equal as well.

Differences in MUSLE soil parameters leading to differences in sensitivities include K_{usle}, soil organic matter, C_{usle}, P_{usle}, and *CFRG* within the first soil layer. A higher K_{usle} factor will lead to more surface erosion. The area-weighted average K_{usle} value was 0.29 for the Sacramento River watershed and 0.32 for the San Joaquin River watershed, indicating that the San Joaquin River watershed is more susceptible for sediment runoff. Additionally, a soil with higher organic matter is less likely to erode than a soil with less organic matter because of sediment cohesion. The area-weighted average for soil carbon content was 1.22% of the soil weight for the Sacramento River watershed and 0.71% of the soil weight for the San Joaquin River watershed. A higher *CFRG* value indicates soils that are more susceptible to sediment erosion. Area-weighted average *CFRG* values were 0.5 for the Sacramento River watershed and 0.8 for the San Joaquin River watershed. Because the San Joaquin River watershed has nearly twice as much agricultural land as the Sacramento River watershed, C_{usle} and P_{usle} values are also higher for the San Joaquin River watershed compared to the Sacramento River watershed.

Implications. The aim of this work is to assess the sensitivity of the Sacramento and San Joaquin River watersheds to climate change using an LHS technique on temperature and precipitation projections. Our sensitivity approach and assumptions are not without fault. As previously mentioned, our LHS scheme assumes that temperature and precipitation are independent. In reality, this is not the case, as temperature and precipitation are inversely related. However, the goal of this study is to assess the sensitivity of the watersheds to changes in temperature and precipitation by using all possible temperature and precipitation projections to bracket the potential ranges of streamflow and agricultural pollutant transport.

Additionally, land-use change is not simulated, and therefore, we assume all climate change projections on current land-use scenarios and management practices. Changes in land use are likely to have significant impact on streamflow and agricultural pollutant fate and transport. However, it is not well known how agricultural land use will change under climate change. The SWAT model used in this study allows changes in irrigation use and fertilization based on changes in soil moisture and plant growth thresholds. This assumes that growers will change their agricultural management techniques based on changes in the soil and crop and is thus a constrained estimate of the changes in irrigation and fertilization. It is important to understand that these inputs may change in the future with changing agricultural management techniques, which may alleviate or increase water quality concerns in a changing climate. Moreover, the results from this study do not include changes in urbanization or agricultural acreage. Increases in urbanization will result in decreases of streamflow either by streamflow or groundwater extraction. An increase in groundwater extraction may decrease stream–aquifer connectivity, resulting in a streamflow baseflow decrease. A decrease in streamflow will further exacerbate the water quality problem, as decreases in streamflow either by streamflow or groundwater extraction may result in increases of contaminant concentrations. Potential future work would include multiple land-use scenarios coupled with climate change scenarios.

Lastly, streamflow in both watersheds are highly controlled by reservoir releases, and the sensitivity of streamflow may not represent the natural sensitivity signal. However, inasmuch as we assume no sediment or nitrate concentrations in the reservoir releases, sediment and nitrate sensitivities are adequately assessed. In conclusion, we present a simple sensitivity assessment of plausible climate change scenarios using current land-use scenarios and management practices, which should therefore be treated with caution.

CONCLUSIONS

This study used the SWAT watershed model to simulate changes in streamflow and agricultural runoff in the Sacramento and San Joaquin River watersheds using LHS from a temperature and precipitation range of 0 to 6.4 °C and ±20%, respectively, compared to the present-day climate. Using 2000 climate change simulations, the 95CI was calculated for streamflow, sediment loads, and nitrate loads. The 95CI results indicate that streamflow and sediment in the Sacramento River watershed are more likely to decrease under climate changes compared to present-day conditions, whereas nitrate runoff was found to increase and decrease by equal amounts. For the San Joaquin River watershed, streamflow slightly decreased under climate change, whereas sediment and nitrate had the tendency to increase compared to the present-day climate. Comparisons of watershed sensitivities indicate that the San Joaquin River watershed is more sensitive to climate change than the Sacramento River watershed. Streamflow, sediment load, and nitrate load *r*-factors were 1.44 and 1.42, 0.59 and 0.68, and 0.69 and 1.02 for the Sacramento and San Joaquin River watersheds, respectively. Climate change sensitivity differences can be attributed to differences in land use and soil properties. The results generated from this study are valuable as a tool for guiding water resource managers and those required to comply with legislation for water quality guidelines to make appropriate decisions on land management and/or measures for environmental protection.

DOI: 10.1002/hyp

REFERENCES

Abbaspour KC, Johnson CA, van Genuchten MT. 2004. Estimating uncertain flow and transport parameters using a sequential uncertainty fitting procedure. *Vadose Zone Journal* **3**: 1340–1352.

Abbaspour KC, Yang J, Maximov I, Siber R, Bogner K, Mieleitner J, Zobrist J, Srinivasan R. 2007. Modelling hydrology and water quality in the pre-alpine/alpine Thur watershed using SWAT. *Journal of Hydrology* **333**: 413–430.

Arnell NW, Liv C. 2001. Hydrology and water resources. In *Climate Change 2001: Impacts, Adaptation and Vulnerability*, McCarthy JJ, Canziani OF, Leary NA, Dokken DJ, White KS (eds). Cambridge University Press: Cambridge, UK; 191–233.

Arnold JG, Srinivasan R, Muttiah RS, Williams JR. 1998. Large area hydrologic modeling and assessment Part I: Model development. *Journal of the American Water Resources Association* **34**: 73–89.

Baalousha H. 2006. Groundwater pollution risk using a modified Latin hypercube sampling. *Journal of Hydroinformatics* **8**: 223–234.

Cayan DR, Maurer EP, Dettinger MD, Tyree M, Hayhoe K. 2008. Climate change scenarios for the California region. *Climatic Change* **87**: 21–42.

Chaplot V. 2007. Water and soil resources response to rising levels of atmospheric CO_2 concentration and to changes in precipitation and air temperature. *Journal of Hydrology* **337**: 159–171.

Cruise JF, Limaye AS, Al-Abed N. 1999. Assessment of impacts of climate change on water quality in the southeastern United States. *Journal of the American Water Resources Association* **35**: 1539–1550.

Department of Water Resources (DWR). 1998. The California Water Plan Update. Bulletin 160–98, Sacramento, California, USA.

Department of Water Resources (DWR). 2007. Land Use Survey Data.

Ferrier RC, Whitehead PG, Sefton C, Edwards AC, Pugh K. 1995. Modelling impacts of land use change and climate change on nitrate-nitrogen in the River Don, North East Scotland. *Water Research* **29**(8): 1950–1956.

Feyrer F, Sommer T, Harrell W. 2006. Importance of flood dynamics versus intrinsic physical habitat in structuring fish communities: Evidence from two adjacent engineered floodplains on the Sacramento River, California. *North American Journal of Fisheries Management* **26**: 408–417.

Ficklin DL, Luo Y, Luedeling E, Zhang M. 2009. Climate change sensitivity assessment of a highly agricultural watershed using SWAT. *Journal of Hydrology* **374**: 16–29.

Ficklin DL, Luo Y, Luedeling E, Gatzke SE, Zhang M. 2010. Sensitivity of agricultural runoff to rising levels of CO_2 and climate change in the San Joaquin Valley watershed of California. *Environmental Pollution* **158**: 223–234.

Ficklin DL, Stewart IT, Maurer EP. 2012a. Projections of 21st century Sierra Nevada local hydrologic flow components using an ensemble of General Circulation Models. *Journal of the American Water Resources Association*. (Accepted)

Ficklin DL, Luo Y, Zhang M. 2012b. Watershed modelling of hydrology and water quality in the Sacramento River watershed, California. Hydrologic Processes (In press).

Gassman PW, Reyes MR, Green CH, Arnold JG. 2007. The Soil and Water Assessment Tool: Historical development, applications, and future research directions. *Trans. of ASABE 50*, 1211–1250.

Guo L, Kelley K, Goh KS. 2007. Evaluation of sources and loading of pesticides to the Sacramento River, California, USA, during a storm event of winter 2005. *Environmental Toxicology and Chemistry* **26**: 2274–2281.

Helton JC, Davis FJ. 2003. Latin hypercube sampling and the propagation of uncertainty in analyses of complex systems. *Reliability Engineering and System Safety* **81**: 23–69.

Iman RL, Helton JC, Campbell JC. 1981. An approach to sensitivity analysis of computer models: Part 1- Introduction, input, variable selection and preliminary variable assessment. *Journal of Quality Technology* **13**: 174–183.

Intergovernmental Panel on Climate Change (IPCC). 2007. *Climate Change 2007: The Physical Science Basis. Contribution of Working Group I to the Fourth Assessment Report of the Intergovernmental Panel on Climate Change*. Cambridge University Press: Cambridge, United Kingdom and New York, NY, USA.

Luo Y, Zhang X, Liu X, Ficklin D, Zhang M. 2008. Dynamic modeling of organophosphate pesticide load in surface water in the northern San Joaquin Valley watershed of California. *Environmental Pollution* **156**: 1171–1181.

Mander U, Kull A, Kuusemets V, Tamm T. 2000. Nutrient runoff dynamics in a rural catchment: Influence of land-use changes, climatic fluctuations and ecotechnological measures. *Ecological Engineering* **14**(4): 405–417.

Maurer EP. 2007. Uncertainty in hydrologic impacts of climate change in the Sierra Nevada, California, under two emissions scenarios. *Climatic Change* **82**: 309–325.

Maurer EP, Duffy PB. 2005. Uncertainty in projections of streamflow changes due to climate change in California. *Geophysical Research Letters* **32**: L03704. DOI: 10.1029/2004GL021462.

McKay MD, Beckman RJ, Conover WJ. 1979. A Comparison of Three Methods of Selecting Values of Input Variables in the Analysis of Output from Computer Code. *Technometrics* **21**: 239–245.

Melching CS. 1992. A comparison of methods for estimating variance in water resources model predictions in Kuo, J. and Lin, G. eds. *Stochastic hydraulics, Proceedings of the Sixth International Association for Hydraulic Research Symposium on Stochastic Hydraulics* Taipeh, Taiwan Water Resources Publications.

Monteith JIL. 1965. *Evaporation and environment*. Academic Press: NY.

Nash JE, Sutcliffe JV. 1970. River flow forecasting through conceptual models: part I. A discussion of principles. *Journal of Hydrology* **10**: 282–290.

National Oceanic and Atmospheric Adminstration (NOAA). National Climatic Data Center. Data Accessed May 15, 2008.

Neitsch SL, Arnold JG, Kiniry JR, Williams JR, King KW. 2005. *Soil and Water Assessment Tool Theroretical Documentation. Version 2005*. Texas Water Resource Institute: College Station, T.X.

Penman HL. 1956. Evaporation: An introductory survey. *Netherlands Journal of Agircultural Science* (1): 9–29, 87–97, 151–153.

Press WH, Teukolsky SA, Vetterling WT, Flannery BP. 1992. *Numerical Recipes: The Art of Scientific Computing*, 2nd edn. Cambridge University Press: Cambridge, England.

Preston BL. 2005. Stochastic Simulation for Climatic Change Risk Assessment and Management. In *MODSIM 2005 International Congress on Modelling and Simulation*, Zerger A, Argent RM (eds). Modelling and Simulation Society of Australia and New Zealand, Inc.: Canberra, December 2005; 170–176. ISBN: 0-9758400-2. http://www.mssanz.org.au/modsim05/papers/preston_1.pdf

Seibert J, McDonnell JJ. 2010. Land-cover impacts on streamflow: a change detection modeling approach that incorporates parameter uncertainty. *Hydrologic Sciences* **55**: 316–332.

Soil Conservation Service (SCS). 1984. *SCS National Engineering Handbook*. U.S. Department of Agriculture: Washington, D.C.

Trenberth KE, Shea DJ. 2005. Relationships between precipitation and surface temperature. *Geophysical Research Letters* **32**: L14703.

Troiano J, Weaver D, Marade J, Spurlock F, Pepple M, Nordmark C, Bartkowiak D. 2001. Summary of well water sampling in California to detect pesticide residues resulting from nonpoint-source applications. *Journal of Environmental Quality* **30**: 448–459.

Werner I, Deanovic LA, Connor V, de Vlaming V, Bailey HC, Hinton DE. 1999. Insecticide-caused toxicity to *ceriodaphnia Dubia* (Cladocera) in the Sacramento – San Joaquin River Delta, California, USA. *Environmental Toxicology and Chemistry* **19**: 215–227.

Williams JR. 1975. Sediment yield prediction with universal equation using runoff energy factor. Proceedings of the Sediment Yield Workshop, USDA Sedimentation Laboratory, Oxford, Mississippi.

Yang J, Reichert P, Abbaspour K, Xia J, Yang H. 2008. Comparing uncertainty analysis techniques for a SWAT application to the Chaohe Basin in China. *Journal of Hydrology* **358**: 1–23.

Yu PS, Yang TC, Chen SJ. 2001. Comparison of uncertainty analysis methods for a distributed rainfall runoff model. *Journal of Hydrology* **244**: 43–59.